Tunable double photonic bandgaps in a homogeneous atomic medium

Shang-qi Kuang,[1,2,3] Ren-gang Wan,[1,2] Jun Kou,[1,2] Yun Jiang,[1,2] and Jin-yue Gao[1,2,*]

[1]*College of Physics, Jilin University, Changchun 130023, China*
[2]*Key Laboratory of Coherent Light, Atomic and Molecular Spectroscopy, Educational Ministry of China, Changchun 130021, China*
[3]*Changchun Institute of Optics, Fine Mechanics and Physics, Chinese Academy of Sciences, Changchun 130033, China*
**Corresponding author: jygao@mail.jlu.edu.cn*

Received March 12, 2010; revised May 11, 2010; accepted June 7, 2010;
posted June 10, 2010 (Doc. ID 125207); published July 9, 2010

Double photonic bandgaps (PBGs) can simultaneously appear when double dark resonances in uniform cold atoms are spatially modulated by a resonance standing-wave. Theoretical calculations show that variable and efficient coherent optical control of the PBGs can be achieved by modulating the coupling field and standing-wave. The structures of double PBGs induced by the atomic coherence effect are better than those obtained in the photonic crystal heterostructures. We anticipate that this scheme has potential applications in optical networks for dual-channel all-optical switching or a dual-frequency optical Bragg reflector. © 2010 Optical Society of America

OCIS codes: 270.1670, 020.1670, 160.5293.

1. INTRODUCTION

Due to the potential application in the construction of various functional devices, photonic crystal (PC) with a periodic modulation of the dielectric constant has been intensively studied [1–3]. In order to achieve the full potential of light channeling and modeling, the incorporation of several different structures of photonic bandgaps (PBGs) in one PC is desirable, and the PC having double PBGs is the basic construction block for this type of device. It has been reported that double PBGs have been observed in the PC heterostructures [4–10] and microstrip structures [11]. However, for the problem of lattice mismatch, the achievement of deep gaps and sharp band edges in the PC heterostructures remains a challenge, and it is difficult to implement a PBG structure by microstrip technology to reflect the optical waves. Meanwhile, for the apparent advantages, tunable PBG structure has attracted much attention [12–16]. Using the thermo- and electro-optic effects of infiltrated liquid crystals [12,13] or nonlinear optical effects in semiconductors [14,15], several schemes have been supplied to tune the PBG structure. Comparing with the modifications of the PBG which do not affect the Brillouin zone, optical induced tunable PBG in uniform ultracold atoms was theoretically presented by employing electromagnetically induced transparency (EIT) [17], in which the Brillouin zone structure can be modulated by the parameters of standing-wave [16]. For the obvious advantages of the solid-state materials, theoretical extensions of the scheme based on the EIT in solid-state materials were also reported [18,19]. Recently, the proposal has been used to calculate the propagation of a light pulse in ultracold atomic gas [20] and color centers in diamond [21].

In this paper, we theoretically present that double PBGs can be induced by atomic coherence effect in a four-level N-type cold atomic system. Due to the spatial periodic modulation of the double dark states [22] induced by a resonant standing-wave, one can obtain a pair of tunable PBGs which are symmetrical around the resonance point of the probe field. Up until now, to reflect different frequencies, various conventional PBG structures with different periods have to be integrated in a PC [4–11], while we find that double PBGs can be formed in the medium with a single dispersion period induced by the standing-wave, and the structures of PBGs are deeper and the band edges are sharper than those obtained in the PC heterostructures. Comparing with the three-level Λ-type atomic configuration [16], our scheme has the advantages that one does not need to use the non-perfect configuration of standing-wave and adjust the misalignment of two counter-propagating beams. This proposal may extend the capability of optical network and has potential applications in the all-optical switching [23–26] and optical Bragg reflector [11].

2. ATOMIC MODEL AND EQUATIONS

The cold atomic system under consideration is shown in Fig. 1, which can be described by a four-level N-type configuration. The transitions $|3\rangle-|1\rangle$, $|3\rangle-|2\rangle$, and $|4\rangle-|2\rangle$ are electric dipole allowed, while the transitions $|2\rangle-|1\rangle$ and $|4\rangle-|1\rangle$ are electric dipole forbidden. A weak probe field ω_p with a Rabi frequency $g=\mu_{31}E_p/2\hbar$, propagating in the z direction, interacts with the transition $|3\rangle-|1\rangle$, while the coupling and standing fields resonantly drive the transitions $|3\rangle-|2\rangle$ and $|4\rangle-|2\rangle$, respectively. The Rabi frequency of the coupling field is $\Omega_c=\mu_{32}E_c/2\hbar$, and the standing-wave along the z direction is formed by the forward and

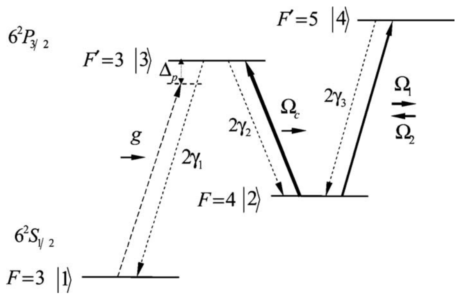

Fig. 1. A schematic diagram of the four-level N-type atomic system.

backward waves with Rabi frequencies $\Omega_1=\mu_{42}E_1/2\hbar$ and $\Omega_2=\mu_{42}E_2/2\hbar$, respectively. Without loss of generality, we take these Rabi frequencies to be real, and $2\gamma_i$ $(i=1,2,3)$ represents the rate of spontaneous emission of the corresponding transition as shown in Fig. 1.

In the framework of the semiclassical theory, using the dipole approximation and the rotating wave approximation, the Hamiltonian H_I of the system in the interaction picture is

$$H_I=-\hbar\Delta_p(|2\rangle\langle 2|+|3\rangle\langle 3|+|4\rangle\langle 4|)-\hbar(g|1\rangle\langle 3|+\Omega_c|2\rangle\langle 3| + \Omega_s^*|2\rangle\langle 4|+\text{H.c.}), \tag{1}$$

where $\Delta_p=\omega_p-\omega_{31}$ is the detuning of the probe field, $\Omega_s=\Omega_1 e^{ik_s z}+\Omega_2 e^{-ik_s z}$, and k_s is the wave vector of the forward and backward fields. The probe field is so weak ($g\ll 2\gamma_1$) that all atoms populate at the ground level $|1\rangle$ $(\rho_{11}=1)$, and levels $|2\rangle$, $|3\rangle$, and $|4\rangle$ remain empty regardless of the intensities of the coupling and standing fields. Therefore, we can ignore all effects which are related to the changes in population and coherence at the transitions ($\rho_{ij}=0$; $i,j=2,3,4$). Including relaxation terms for the closed system, the equations of motion for the density matrix of the four-level system can be written as

$$\dot{\rho}_{31}=(i\Delta_p-\gamma_{31})\rho_{31}+i\Omega_c\rho_{21}+ig,$$

$$\dot{\rho}_{21}=(i\Delta_p-\Gamma_{21})\rho_{21}+i\Omega_c\rho_{31}+i\Omega_s^*\rho_{41},$$

$$\dot{\rho}_{41}=(i\Delta_p-\gamma_{41})\rho_{41}+i\Omega_s\rho_{21}, \tag{2}$$

where $\gamma_{31}=\gamma_1+\gamma_2$, $\gamma_{41}=\gamma_3$, and Γ_{21} is the dephasing rate for the transition $|2\rangle-|1\rangle$ due to atomic collisions. For simplicity, we assume $\gamma_1=\gamma_2=\gamma_3=\gamma/2$ and then obtain the steady solution of the element ρ_{31} as

$$\frac{\rho_{31}}{g}=-\frac{1}{\Delta_p+i\gamma+(\Delta_p+i\gamma/2)\Omega_c^2/\mathcal{M}}, \tag{3}$$

where $\mathcal{M}=(i\Delta_p-\gamma_{21})(i\Delta_p-\gamma/2)+\Omega_s^2$. Form Eq. (3), one can obtain the linear susceptibility $\chi(\Delta_p,z)$ and refractive index $\epsilon(\Delta_p,z)$ experienced by the probe field as

$$\epsilon=1+\chi=1+3\pi\mathcal{N}\gamma\frac{\rho_{31}}{g}. \tag{4}$$

Here $\mathcal{N}=N_0(\lambda_p/2\pi)^3$ is the scaled average atomic density, N_0 represents the atomic density, and λ_p is the wavelength of the probe field. It is worthwhile to point out that the standing-wave intensity profile and its space periodicity do not alter the space distribution of cold atoms, owing to the weak probe field and the standing-wave with a resonance frequency.

Due to the spatial periodic modulation induced by the standing-wave, the weak probe field propagates as in a one-dimensional grating with a periodicity $a=\lambda_s/2$ [27], which is the half-wavelength of the standing-wave. We divide the length a into m equal parts and calculate the 2×2 unimodular transfer matrix of each part [28]. After multiplying the matrices of all parts in a period, we numerically calculated the transfer matrix $M(\Delta_p)$ which represents the propagation of the probe field through a single period. The translational invariance of the periodic medium is fulfilled by imposing the Bloch condition on the photonic eigenstates,

$$\begin{pmatrix} E^+(z+a) \\ E^-(z+a) \end{pmatrix}=M(\Delta_p)\begin{pmatrix} E^+(z) \\ E^-(z) \end{pmatrix}=\begin{pmatrix} e^{i\kappa a}E^+(z) \\ e^{i\kappa a}E^-(z) \end{pmatrix}, \tag{5}$$

where E^+ and E^- are the electric field amplitudes of the forward and backward (Bragg reflected) propagating probes, respectively, and $\kappa=\kappa'+i\kappa''$ is the Bloch complex wave vector of the corresponding probe photonic states. The one-dimensional grating structure is obtained from the solution of the corresponding determinantal equation $e^{2i\kappa a}-\text{Tr}[M(\Delta_p)]e^{i\kappa a}+1=0$ (det $M=1$) and we note both κ and $-\kappa$ are the solutions of the equation. As a result, we can simply have

$$\kappa a=\pm\cos^{-1}\left[\frac{\text{Tr}[M(\Delta_p)]}{2}\right]. \tag{6}$$

The above discussion is related to Bloch modes for the probe field in an infinite periodic stack, while one must pay attention to the propagation through a sample with a finite length in real experiments [29]. Therefore, we consider the corresponding reflectivity and transitivity spectra of the probe field which propagates through a sample of thickness $L=Na$, where N is the number of the standing-wave periods. The total transfer matrix $M_{(N)}$ of a sample with thickness $L=Na$ ($N\gg 1$) is given in terms of a single period transfer matrix M as $M_{(N)}=M^N$. Because M is unimodular, the following closed expression for $M_{(N)}$ holds true:

$$M_{(N)}=\frac{\sin(N\kappa a)}{\sin(\kappa a)}M-\frac{\sin[(N-1)\kappa a]}{\sin(\kappa a)}I, \tag{7}$$

where I is the unity matrix. With the compact expression, we have the ability to calculate the reflection (R_N) and transmission (T_N) amplitudes for the length L in terms of the complex Bloch wave vector κ and the element M_{ij} of the matrix M,

$$R_N=\frac{M_{N(12)}}{M_{N(22)}}=\frac{M_{12}\sin(N\kappa a)}{M_{22}\sin(N\kappa a)-\sin[(N-1)\kappa a]},$$

$$T_N=\frac{1}{M_{N(22)}}=\frac{\sin(\kappa a)}{M_{22}\sin(N\kappa a)-\sin[(N-1)\kappa a]}. \tag{8}$$

Using Eq. (8), we can obtain the reflectivity, transmissivity, and absorption of the probe field by calculating $|R_N|^2$, $|T_N|^2$, and $A=1-|R_N|^2-|T_N|^2$, respectively.

3. RESULTS AND DISCUSSION

In the following, we demonstrate the calculated results which correspond to the transitions of cold Cs atoms as shown in Fig. 1, and chose $2\gamma/2\pi=5.234$ MHz and $\Gamma_{21}/2\pi\approx 1$ kHz. At first, we present the result of κa for a configuration of the perfect standing-wave $\Omega_1=\Omega_2=20\gamma$ in Fig. 2(a). An investigation of Fig. 2(a) shows that two forbidden gaps open up in the frequency range for which $\kappa' =\pi/a$ and $\kappa''\neq 0$, and the PBGs are symmetrical around a resonance point. It is worthwhile to point out that double PBGs arise in the homogeneous cold atoms with a single dispersion period induced by the standing-wave, which is different from other proposals using various conventional PBG structures with different periods in the PC heterostructures [4–10]. In order to interpret this result, we supply an analysis in the dressed-state picture of the system. The interaction Hamiltonian for the atoms which are driven by the coupling and standing fields can be written as

$$H_I=-\hbar\begin{pmatrix} 0 & \Omega_c & \Omega_s^* \\ \Omega_c & 0 & 0 \\ \Omega_s & 0 & 0 \end{pmatrix}. \tag{9}$$

From Eq. (9), the three dressed sub-levels, generated by the coupling and standing fields, are

$$|+\rangle=\frac{\sqrt{2}}{2}\left(|2\rangle+\frac{\Omega_c}{\alpha_-}|3\rangle+\frac{\Omega_s}{\alpha_-}|4\rangle\right),$$

$$|-\rangle=\frac{\sqrt{2}}{2}\left(|2\rangle+\frac{\Omega_c}{\alpha_+}|3\rangle+\frac{\Omega_s}{\alpha_+}|4\rangle\right),$$

$$|0\rangle=-\frac{\Omega_s^*}{\alpha_+}|3\rangle+\frac{\Omega_c}{\alpha_+}|4\rangle, \tag{10}$$

where $\alpha_\pm=\pm\sqrt{\Omega_c^2+\Omega_s^2}$ and $\alpha_0=0$ are the corresponding eigenvalues of the dressed states. It is obvious that the dressed states change periodically in space, and the eigenvalues which correspond to the absorption peaks of the probe field have the same period. Due to the interference effects of the dressed states, one can achieve double dark resonances [22], which lead to a pair of transparency points at the frequencies $\Delta_p=\pm|\Omega_s|$. With the purpose to further clarify this underlying physics, we check the absorptions of the probe field at different points along z with different intensities of the standing-wave in Fig. 2(b). In Fig. 2(b), one can see that one dark resonance changes to double dark resonances as one moves along z from nodes to antinodes of the standing-wave, and this change has a periodic fashion which is the same as the intensity pattern of the standing-wave. Therefore, the probe absorption is modified periodically near the double dark resonances, and the dispersion is also modulated in the same period due to the Kramer–Kronig relations [30]. As a result, the probe field propagates as in a multi-layer periodic structure and double PBGs are expected to occur.

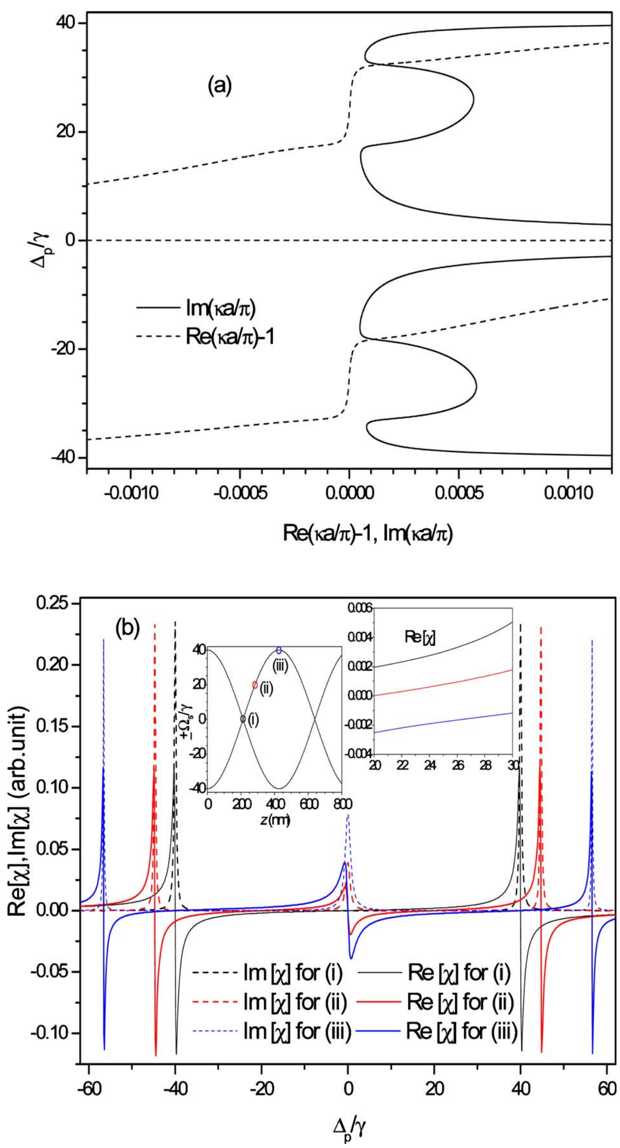

Fig. 2. (Color online) (a) Bandgap structure for the probe field in a homogeneous sample of ultracold Cs ($N_0=5\times 10^{12}$ cm^{-3}) in the presence of coupling field $\Omega_c=40\gamma$ and a periodic modulation induced by a standing-wave $\Omega_1=\Omega_2=20\gamma$. Real and imaginary parts of Bloch wave vector of probe field are shown. (b) Real and imaginary parts of the susceptibility χ at probe frequency Δ_p in the control of the coupling field $\Omega_c=40\gamma$ and in different positions of the standing-wave: (i) $\Omega_s=0$; (ii) $\Omega_s=20\gamma$; (iii) $\Omega_s=40\gamma$. The insets show the corresponding intensity profile of standing-wave and a magnified part of the same part of real part of susceptibility χ.

Secondly, we supply the reflectivity and transmissivity of the probe field which experiences ultracold atomic gas with a length of $L=2$ mm in Fig. 3. In the dressed-state picture of the coupling field Ω_c, standing-wave Ω_s, and levels $|2\rangle$, $|3\rangle$, and $|4\rangle$, the probe field has three absorption points which correspond to the three eigenvalues of the dressed states. The first absorption point is at the resonance frequency, and the other two absorption points locate at frequencies $\Delta_p=\sqrt{\Omega_c^2+\Omega_s^2}$ and $\Delta_p=-\sqrt{\Omega_c^2+\Omega_s^2}$. Therefore, the absorption of the probe field for large detuning is not negligible, and the sum of transmissivity and reflectivity in Fig. 3 is not equal to 1. Owing to efficient constructive interference of in-phase contributions from multiple reflections between adjacent layers, the reflectivity of probe around the resonance point becomes large. The structures of PBGs agree with the results in

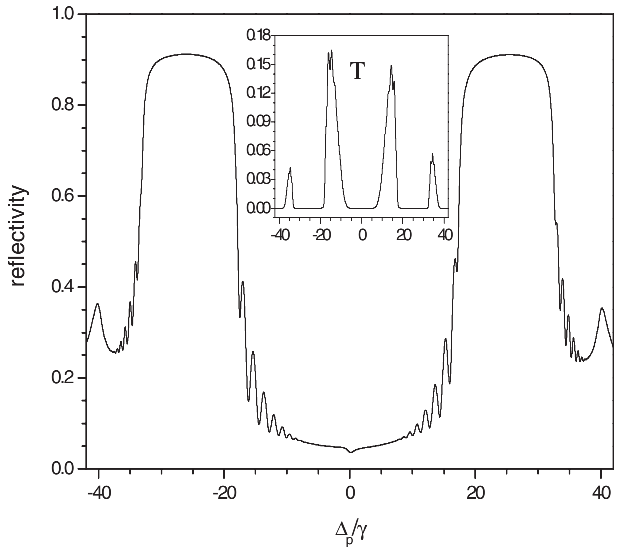

Fig. 3. Reflectivity of induced bandgap in a sample of length $L=2$ mm. The inset shows the corresponding transmissivity. All other parameters are the same as in Fig. 2(a).

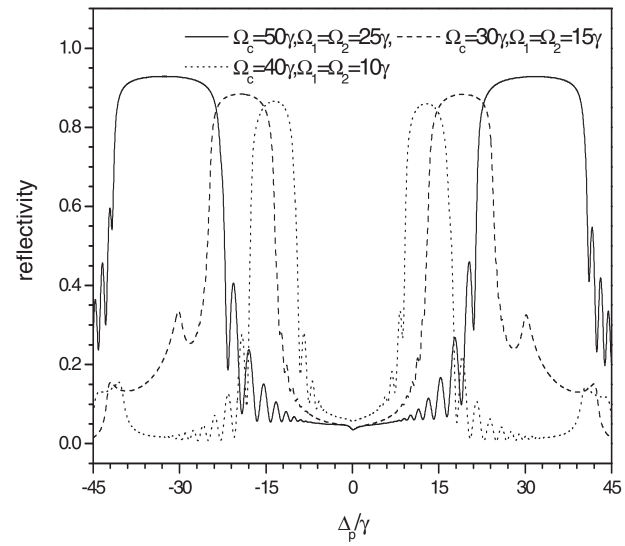

Fig. 4. Tuning of the bandgap reflectivity for different intensities of the coupling and standing fields. The sample has a length $L=2$ mm. All other parameters are the same as in Fig. 2(a).

Fig. 2(a), and the bandgaps are all contained in the transparency windows in Fig. 2(b). We demonstrate that atomic coherence effect can induce double PBGs with a good structure, which is difficult to observe in the PC heterostructures due to the problem of lattice mismatch [4–10]. In our assumption, the configuration of the standing-wave is perfect ($\Omega_1=\Omega_2$) which is different from the specific standing-wave configuration in the three-level Λ-type atomic system ($\Omega_2\approx 0.8\Omega_1$) [16]. The reason is that there is no absorption due to the EIT at the nodes of the perfect standing-wave in our system, while it has to use quasi-nodes of the non-perfect standing-wave to overcome the detrimental effects of absorption in the three-level atomic systems. Because the PBGs locate at opposite frequency regions around the resonance point, we do not need to adjust the misalignment of two counter-propagating beams to change the frequency region of the PBG from above to below resonance or vice versa. Based on these considerations, the experimental simplicity and stability of our scheme are better than those of the three-level atomic system [16]. It should be noted that our scheme is related to the Bragg scheme in the four-level atomic system [31], in which the frequency of the standing-wave is far detuning. In the four-level atomic system, the spatial periodic modulation of the probe dispersion is induced by the EIT enhanced nonlinear index, and the perfect PBG appears in the transparency window where the absorption is absolutely canceled, while in our scheme the spatial modulation of probe dispersion created by a resonant standing-wave is related to the spatial modulation of nonlinear absorption, and there are double PBGs induced by double dark states.

We further present in Fig. 4 how to adjust the positions and widths of PBGs by changing intensities of the coupling and standing fields. With a stronger coupling field, the frequency range of the PBG becomes larger, and the frequency position becomes more far away from the resonance point. By adjusting the intensity of the standing-wave, one can find the same results as the coupling field. These results can be understood that the transparency window of dark resonance has a wider frequency range and the transparency point becomes more far away from the resonance point when the fields become stronger. It also demonstrates that for larger intensities of the coupling and standing fields, one can obtain a larger reflectivity of the probe field and a better gap structure, which are induced by the more highly effective quantum coherence and interference effects of strong fields.

Because this scheme can obtain double PBGs simultaneously, one can switch off a pair of light signals with different frequencies. Since the frequency region of the PBG is contained in the transparency window, in the absence of the backward field, double light signals can pass the medium with a small loss. As the standing-wave is formed, both of the signals would be reflected; therefore, our scheme is suitable to form a dual-channel all-optical switching [26]. Owing to the reflectivity of probe as shown in Fig. 4, our proposal can also be used as a tunable dual-frequency optical Bragg reflector [11]. For the general physics underlying, it should be straightforward to consider the extension of our scheme to achieve double PBGs in condensed matter systems [32], which may offer more flexibilities and functions in practical devices.

4. CONCLUSIONS

In conclusion, we theoretically present that double PBGs can be simultaneously induced by the atomic coherence effects in ultracold atomic gas. A variable and efficient coherent optical control of PBGs can be achieved by the modulating the intensities of coupling and standing fields. The structure of double PBGs induced by a single dispersion period in our scheme is better than that obtained in the PC heterostructures, and our calculations hold more potential for effective control of the light-matter interaction and its applications in optical networks.

ACKNOWLEDGMENTS

This work is supported by the National Natural Science Foundation of China (NSFC) (Grants No. 10334010 and No. 10774059), the doctoral program foundation of institution of High Education of China, and the National Basic Research Program (Grant No. 2006CB921103).

REFERENCES AND NOTES

1. E. Yablonovitch, "Inhibited spontaneous emission in solid-state physics and electronics," Phys. Rev. Lett. **58**, 2059–2062 (1987).
2. S. John, "Strong localization of photons in certain disordered dielectric superlattices," Phys. Rev. Lett. **58**, 2486–2489 (1987).
3. J. D. Joannopoulos, R. D. Mcade, and J. N. Win, *Photonic Crystals: Molding the Flow of Light* (Princeton U. Press, 1995).
4. S. G. Romanov, H. M. Yates, M. E. Pemble, and R. M. De La Rue, "Opal-based photonic crystal with double photonic bandgap structure," J. Phys. Condens. Matter **12**, 8221–8229 (2000).
5. M. Egen, R. Voss, B. Griesebock, and R. Zentel, "Heterostructures of polymer crystal films," Chem. Mater. **15**, 3786–3792 (2003).
6. N. Gaponik, A. Eychmüller, A. L. Rogach, V. G. Solovyev, C. M. Sotomayor Torres, and S. G. Romanov, "Structure-related optical properties of luminescent hetero-opals," J. Appl. Phys. **95**, 1029–1035 (2004).
7. M. Bardosova, M. E. Pemble, I. M. Povey, R. H. Tredgold, and D. E. Whitehead, "Enhanced Bragg reflections from size-matched heterostructure photonic crystal thin films prepared by the Langmuir–Blodgett method," Appl. Phys. Lett. **89**, 093116 (2006).
8. R. V. Nair and R. Vijaya, "Three-dimensionally ordered photonic crystal heterostructures with a double photonic stop band," J. Appl. Phys. **102**, 056102 (2007).
9. G. Q. Liu, Z. S. Wang, Y. B. Liao, H. H. Hu, and Y. Chen, "High-quality photonic crystal heterostructures fabricated by a modified self-assembly method," Appl. Opt. **48**, 2480–2484 (2009).
10. Z. Q. Liu, T. H. Feng, Q. F. Dai, L. J. Wu, and S. Lan, "Fabrication of high-quality three-dimensional photonic crystal heterostructures," Chin. Phys. B **18**, 2383–2388 (2009).
11. M. A. G. Laso, T. Lopetegi, M. J. Erro, D. Benito, M. J. Garde, and M. Sorolla, "Multiple-frequency-tuned photonic bandgap microstrip structures," IEEE Microw. Guid. Wave Lett. **10**, 220–222 (2000).
12. K. Busch and S. John, "Liquid-crystal photonic-band-gap materials: The tunable electromagnetic vacuum," Phys. Rev. Lett. **83**, 967–970 (1999).
13. D. Kang, J. E. Maclennan, N. A. Clark, A. A. Zakhidov, and R. H. Baughman, "Electro-optic behavior of liquid-crystal-filled silica opal photonic crystals: Effect of liquid-crystal alignment," Phys. Rev. Lett. **86**, 4052–4055 (2001).
14. X. Y. Hu, Q. Zhang, Y. H. Liu, B. Y. Cheng, and D. Z. Zhang, "Ultrafast three-dimensional tunable photonic crystal," Appl. Phys. Lett. **83**, 2518–2520 (2003).
15. H. W. Tan, H. M. van Driel, S. L. Schweizer, R. B. Wehrspohn, and U. Gösele, "Nonlinear optical tuning of a two-dimensional silicon photonic crystal," Phys. Rev. B **70**, 205110 (2004).
16. M. Artoni and G. C. La Rocca, "Optically tunable photonic stop bands in homogeneous absorbing media," Phys. Rev. Lett. **96**, 073905 (2006).
17. S. Harris, "Electromagnetically induced transparency," Phys. Today **50**(7), 36–42 (1997).
18. Q. Y. He, J. H. Wu, T. J. Wang, and J. Y. Gao, "Dynamic control of the photonic stop bands formed by a standing wave in inhomogeneous broadening solids," Phys. Rev. A **73**, 053813 (2006).
19. Q. Y. He, Y. Xue, M. Artoni, G. C. La Rocca, J. H. Xu, and J. Y. Gao, "Coherently induced stop-bands in resonantly absorbing and inhomogeneously broadened doped crystals," Phys. Rev. B **73**, 195124 (2006).
20. J. H. Wu, M. Artoni, and G. C. La Rocca, "Controlling the photonic band structure of optically driven cold atoms," J. Opt. Soc. Am. B **25**, 1840–1849 (2008).
21. J. H. Wu, G. C. La Rocca, and M. Artoni, "Controlled light-pulse propagation in driven color centers in diamond," Phys. Rev. B **77**, 113106 (2008).
22. M. D. Lukin, S. F. Yelin, M. Fleischhauer, and M. O. Scully, "Quantum interference effects induced by interacting dark resonances," Phys. Rev. A **60**, 3225–3228 (1999).
23. M. Scalora, J. P. Dowling, C. M. Bowden, and M. J. Bloemer, "Optical limiting and switching of ultrashort pulses in nonlinear photonic band gap materials," Phys. Rev. Lett. **73**, 1368–1371 (1994).
24. D. A. Mazurenko, R. Kerst, J. I. Dijkhuis, A. V. Akimov, V. G. Golubev, D. A. Kurdyukov, A. B. Pevtsov, and A. V. Sel'kin, "Ultrafast optical switching in three-dimensional photonic crystals," Phys. Rev. Lett. **91**, 213903 (2003).
25. A. W. Brown and M. Xiao, "All-optical switching and routing based on an electromagnetically induced absorption grating," Opt. Lett. **30**, 699–701 (2005).
26. G. Wang, Y. Xue, J. H. Wu, S. S. Liu, Z. H. Kang, and J. Y. Gao, "Dual-channel all-optical wavelength conversion switching by four-wave mixing," Opt. Express **17**, 23332–23337 (2009).
27. In this paper, the wavelengths of the probe, coupling, and standing fields are $\lambda_p = 852.335$ nm, $\lambda_c = 852.357$ nm, and $\lambda_s = 852.356$ nm, respectively.
28. M. Artoni, G. C. La Rocca, and F. Bassani, "Resonantly absorbing one-dimensional photonic crystals," Phys. Rev. E **72**, 046604 (2005).
29. K. Sakoda, *Optical Properties of Photonic Crystals* (Springer, 2001).
30. J. D. Jackson, *Classical Electrodynamics*, 2nd ed. (Wiley, 1975).
31. A. André and M. D. Lukin, "Manipulating light pulses via dynamically controlled photonic band gap," Phys. Rev. Lett. **89**, 143602 (2002).
32. A. V. Turukhin, V. S. Sudarshanam, M. S. Shahriar, J. A. Musser, B. S. Ham, and P. R. Hemmer, "Observation of ultraslow and stored light pulses in a solid," Phys. Rev. Lett. **88**, 023602 (2001).